Thermal Conductivity Measurement of the Interaction Layer between UMo and Al Produced by High-Energy Heavy Ion Irradiation

Yinbin Miao[a,*], Lakshmi Amulya Nimmagadda[b], Manjunath C. Rajagopal[b], Kun Mo[a], Jingyi Shi[c], Bei Ye[a], Laura Jamison[a], Yeon Soo Kim[a], Winfried Petry[c], Sanjiv Sinha[b,d], Abdellatif M. Yacout[a]

[a]*Argonne National Laboratory, Lemont, IL 60439, United States*
[b]*Mechanical Science & Engineering Department, University of Illinois, Urbana, IL 61801, United States*
[c]*Technical University of Munich, 80333 Munich, Germany*
[d]*Micro & Nanotechnology Laboratory, University of Illinois, Urbana, IL 61801, United States*

Abstract

Here, we report the first direct thermal conductivity measurement results for Al-UMo interaction layer (IL), which is typically observed in UMo/Al dispersion fuel plates under irradiation. The investigated IL was formed by irradiating Al coated UMo substrate using 80 MeV iodine ions at 180°C up to 3.03×10^{17} ions/cm^2 fluence. Microstructural characterization indicated that the induced IL is amorphous with an approximately $(U_{0.8},Mo_{0.2})Al_{5.3}$ stoichiometry, which is similar to that formed under in-pile irradiation. Focused ion beam (FIB) was used to prepare nine specimens of various lengths from the IL that could be suspended across a microfabricated device for thermal conductivity measurement. The measured thermal conductivity values of the IL were significantly lower than the values for both the original UMo fuel and the Al. The successful measurement of the Al-UMo IL provides valuable information for the development and qualification of UMo/Al dispersion fuels for research and test reactor conversion applications, and further demonstrates the promising capabilities of utilizing the suspended bridge method in nuclear fuel research.

Keywords: high-energy ion irradiation, thermal conductivity, interaction layer, UMo fuel, research reactors

*Tel: +1 (630)252-7448. Email: ymiao@anl.gov (Y. Miao)

1. Introduction

Development of new nuclear fuels for research and test reactors in order to reduce the enrichment of uranium to below 20% has been a global campaign for decades [1]. This can only be achieved by compensating the loss in enrichment by an adequate increase in uranium density [2]. Therefore, uranium alloys and compounds with a greater uranium density compared to conventional oxide fuels, such as U_3Si_2 [3], have been sucessfully applied in the conversion of some reactors. To convert those research and test reactors with higher power requirements, nuclear fuel materials with even higher uranium density must be examined. Among the possible materials, UMo alloy has been regarded as a promising candidate for next-generation high-performance research and test reactors given its advantageous uranium density [4, 5]. UMo alloy can be used in both dispersion and monolithic forms [6]. In the dispersion fuel form, spherical UMo alloy particles fabricated by atomization are dispersed into an Al matrix (UMo/Al fuel), which is clad in Al alloy in plate-type fuel.

The development and qualification of UMo/Al fuel requires the accurate and reliable prediction of its performance under operating conditions in reactors. Materials experience harsh conditions in nuclear reactors, such as high radiation dose, and are, therefore, subject to significant microstructural modifications. The changes in structure at the microscopic level alter the macropscopic materials properties, leading to variable fuel performance. Specifically, the thermal conductivity of fuel materials usually experiences degradation under irradiation. Thermal conductivity is one of the most important thermophysical properties of the fuel, and has a significant impact on fuel performance. Hence, better understanding of the radiation-induced microstructural modification and corresponding changes in fuel performance, especially thermal conductivity, which is crucial for the development of UMo/Al fuel form.

According to in-pile irradiation campaigns and post-irradiation examinations (PIEs) of UMo/Al fuels, one of the most prominent microstructural modifications observed under irradiation is the formation of interaction layer (IL) between the UMo fuel particles and Al matrix [7, 8, 9]. This IL was found to be (U,Mo)Al_x with the stoichiometry parameter x ranging from 3 to 8 [10, 11]. The Al-UMo IL is usually amorphous and thus lacks a crystalline structure [12]. The formation of the

IL has been estimated to make a major contribution to the thermal conductivity degradation of the UMo/Al fuel plate and thus is of great importance to its fuel performance evaluation [13, 14]. However, the thermal conductivity of the Al-UMo IL has not been directly measured, mainly due to the limited length scale. Because the thermal conductivity of IL has been an unknown, various assumptions were made regarding the evaluation of UMo/Al fuel system, leading to large uncertainty in those evaluation [15, 13, 14].

Recent developments in nanomaterial science enabled measuring radiation-induced structures with lower-length scales, providing a solution for the lack of thermal conductivity measurements on the IL. Miao et al. [16] measured the thermal conductivity of thin rod specimens prepared from both bulk stainless steel and a single UMo fuel particle, demonstrating the feasibility of utilizing the suspended bridge method [17, 18, 19] for nuclear material research. In this study, the applications of the suspended bridge method were further explored by directly measuring the thermal conductivity of the Al-UMo IL for the first time. The Al-UMo IL was induced by irradiating an Al coated UMo foil using high-energy heavy ion irradiation. High-energy heavy ions produced by accelerators are capable of simulating some of the energetic fission fragments, which cause the majority of radiation damage in nuclear fuel materials. Using heavy ion irradiation, a series of characteristic radiation-induced microstructure features observed in in-pile irradiated nuclear fuels were successfully replicated [20, 21, 22, 23, 24, 25, 26, 27, 28, 29]. Therefore, an ion irradiated depleted uranium sample was used instead of in-pile irradiated low-enriched uranium (LEU) sample at this early stage of research in order to reduce the radiation hazards involved (e.g., actinides and fission products formed in reactors) and to facilitate the characterization of the irradiated samples. Characterization of the microstructure of the irradiated Al-UMo IL demonstrated the similarity with the IL observed in in-pile irradiated UMo/Al fuels.

2. Experiments

2.1. Formation of Al-UMo Interaction Layer

Samples of a layered structure consisting of an UMo substrate with an Al coating were prepared at the Technical University of Munich (TUM) using physical vapor deposition (PVD).

The production process is given in Ref. [30]. A U-10Mo monolithic foil with a thickness of 330 μm was used as the substrate in this model system. The substrate foil was then coated by a 13 μm thick Al layer using DC magnetron sputtering, which is a PVD process. This Al-coated UMo sample was used in this study, because the representative sample geometry provides better control of the irradiation conditions, compared to using spherical powder. It is worth mentioning that the sputtered Al layer usually has a slightly lower density (~2.5 g/cm^3) compared to the theoretical density of Al (2.7 g/cm^3). A square specimen 10 mm × 10 mm in size was sectioned from the Al-coated UMo foil (see Fig. 1(a)). In order to form Al-UMo IL within the specimen for further characterizations, high-energy heavy ion irradiation was employed to create an IL that is comparable to those observed in in-pile irradiated UMo/Al fuels. The specimen was irradiated with 80 MeV iodine-127 ions, which replicate a representative fission product with typical kinetic energy, at the Maier-Leibnitz Laboratory (MLL) accelerator at TUM . The Al coated UMo foil was irradiated at 180±5°C up to 3.03×10^{17} ions/cm^2 fluence, which is equivalent to approximately 3.18×10^{20} fissions/cm^3 fission density for in-pile irradiated UMo/Al fuel [31]. The irradiation temperature was selected because it is within the typical temperature range of plate-type dispersion fuel meat under operating conditions [32]. As shown in Fig. 1(b), using the burn mark left by the ion beam on the sample surface as an indication of the peak dose, the irradiated specimen was embedded in epoxy and polished to expose the cross section with the peak irradiation dose so that the Al-UMo IL can be directly investigated (Fig. 1(c) and (d)) [29].

2.2. Microstructure Characterizations

The cross section of the ion-irradiated Al coated UMo monolithic model system was first investigated using scanning electron microscopy (SEM). An FEI Strata 400 DualBeam system equipped with a field emission gun (FEG) electron source was used for surface characterization of the cross section, with a focus on the location irradiated by the ion beam center. In order to further investigate the detailed microstructure of the Al-UMo IL, focused ion beam (FIB) technique available in the same FEI Strata 400 DualBeam system was used to mill and lift out a slice of the sample containing Al, UMo and IL layers. The lift-out slice was then mounted on a copper Omniproble ~~TEM (transmission electron microscopy)~~transmission electron microscope

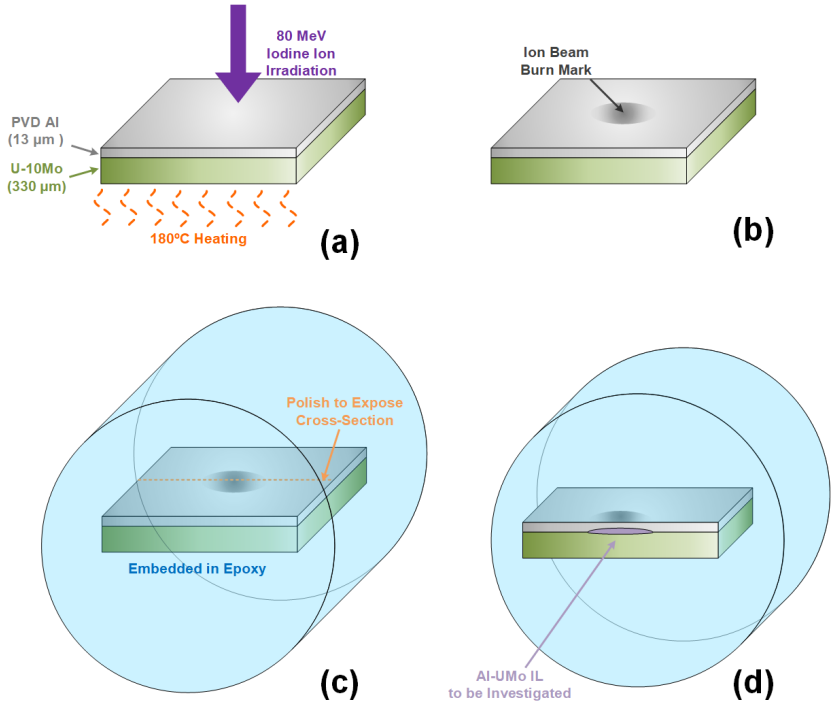

Figure 1: Schematics showing the procedures to induce Al-UMo interaction layer investigated in this study: (a) an Al coated UMo foil irradiated by ^{127}I ions at 180°C; (b) the irradiated specimen with burn mark; (c) the irradiated specimen embedded in epoxy; (d) polished specimen with cross section corresponding to ion beam center exposed.

(TEM) grid and polished using Ga ion beam so that energy dispersive X-ray spectroscopy in the SEM (SEM-EDS) could be used to quantitatively measure the elemental composition of the Al-UMo IL. The lift-out slice was further thinned by FIB to ~50 nm for TEM characterization, which was performed with Argonne National Laboratory's Intermediate Voltage Electron Microscope (IVEM-Tandem) working at 300 kV. The TEM characterization focused on the determination of the Al-UMo IL's microstructure is reported in Section 3.1.

2.3. Suspended Bridge Method

In order to measure the thermal conductivity of the Al-UMo IL, which is only a few microns in thickness, the suspended bridge method was adopted in this study. This method was first developed by Shi et al. [17] and was used to measure the thermal conductivity of one-dimensional or nearly-one-dimensional nanomaterials such as nanotubes, nanowires and nanobelts [18, 19]. Recently, this method was successfully applied by Miao et al. [16] to measure the thermal conductivity of nuclear materials of reduced length scale. The fundamental principle of this technique is detailed in Fig. 2 (a) with variables used to calculate the thermal conductivity of the sample drawn in the schematic. A nanoribbon specimen is mounted bridging two suspended membrane platforms made of electrically and thermally insulating materials (e.g. silicon nitride). Each membrane platform is supported by six thin beams. Platinum patterned lines are micro-fabricated on the two platforms as resistors so that one of the platforms (heating platform) can be heated by the resistor to allow heat to flow to the other platform (sensing platform) through the nanoribbon specimen. The temperatures of both platforms, as well as the heat generated on the heating platform and supporting beams, can be measured and used to deduce the thermal conductance of the bridge specimen (G_{bs}), as shown in Equations 1 and 2.

$$G_b = \frac{Q_h + Q_L}{(T_h - T_0) + (T_s - T_0)}; \tag{1}$$

$$G_{bs} = G_b \frac{T_s - T_0}{T_h - T_s}. \tag{2}$$

Here, T_h, T_s, and T_0 are temperatures of the heating platform, sensing platform, and environment

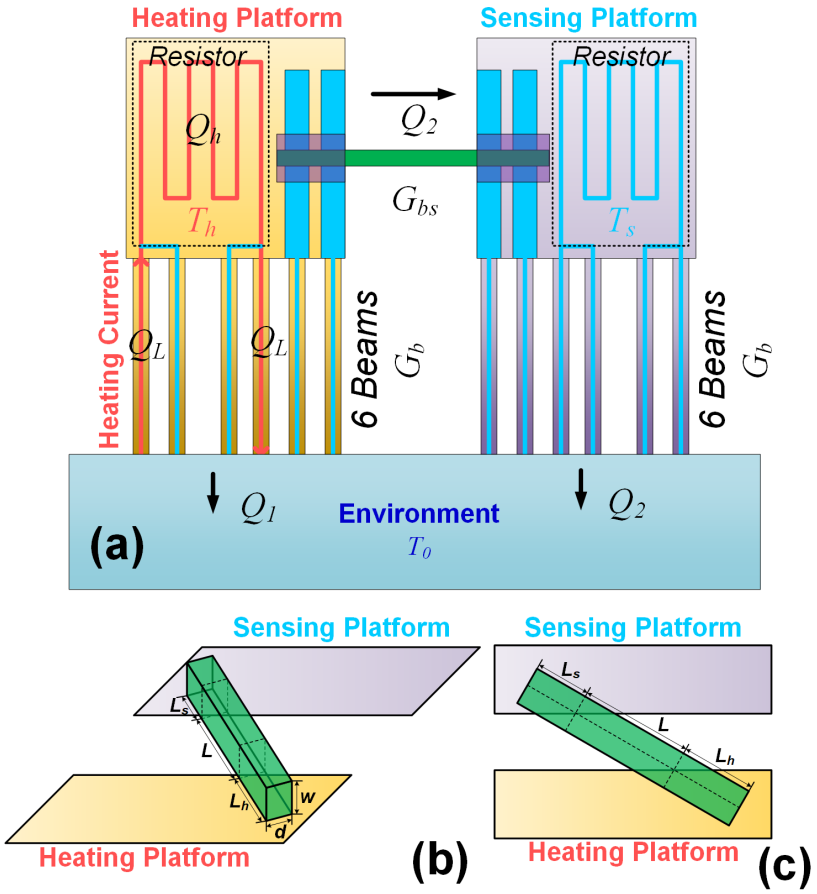

Figure 2: Principle of the suspended bridge thermal conductivity measurement and involved dimensions: (a) a schematic showing the measurement platform; (b) a pictorial drawing showing the dimensions; (c) a top-view drawing showing the dimensions.

(in the cryostat), respectively; G_b is the total thermal conductance of the six beams supporting either platform; and Q_h and Q_L are the electric heating power of the patterned platinum resistor on the heating platform and either of the supporting beams, where the heating current flows through, respectively. A detailed description of the method can be found in Miao et al.'s paper [16]. In order to eliminate the heat transfer effects from convection and thermal radiation, this measurement technology needs to be performed under vacuum and is currently capable of measuring thermal conductivity from cryogenic temperature up to approximately 400 K.

2.4. Sample Preparation

In this study, the Al-UMo IL formed in the ion-irradiated Al coated UMo foil model system, described in Section 2.1, was investigated. The thin rod specimens for thermal conductivity measurement were prepared using the FEI Strata 400 DualBeam system. An approximately 20 μm $\times$ 10 μm $\times$ 1.5 μm thin slice was ion milled and lifted out from the IL region near the ion beam center location (Fig. 3(a)). The lift-out was then transferred to a copper Omniprobe TEM grid and then thinned to ~300 nm (Fig. 3(b)). The measured sample is approximately in the center of the IL formed on the Al-UMo interface. Both sides of the thinned slice were cleaned using 5 kV and 2 kV Ga ions to minimize the extra radiation effects induced by FIB. The Omniprobe TEM grid with the slice was then tilted by 90° so that the FIB thinned and polished surfaces could be vertical to the ion beam. Thin rods with rectangular cross sections were then cut from the slice using FIB and transferred to the micro-fabricated measurement platform using a tungsten Omniprobe tip (Fig. 3(c)). Pt deposition enabled by the gas injection system (GIS) of the FIB was used to mount the thin rods onto the measurement platforms as bridges to minimize the thermal resistance between the thin rods and the platforms (Fig. 3(d)). Nine thin rods with various bridge lengths, which approximately range from 3 μm to 15 μm, were prepared in this study and mounted. The range of bridge lengths is needed in order to correct for the contact thermal resistance between the thin rod specimens and the two platforms, which was found to be comparable to the intrinsic thermal resistance of the thin rod specimens. The different bridge lengths were achieved by putting the thin rod specimens onto the platforms at different angles. A detailed procedure to correct for the contact thermal resistance is described in the next subsection.

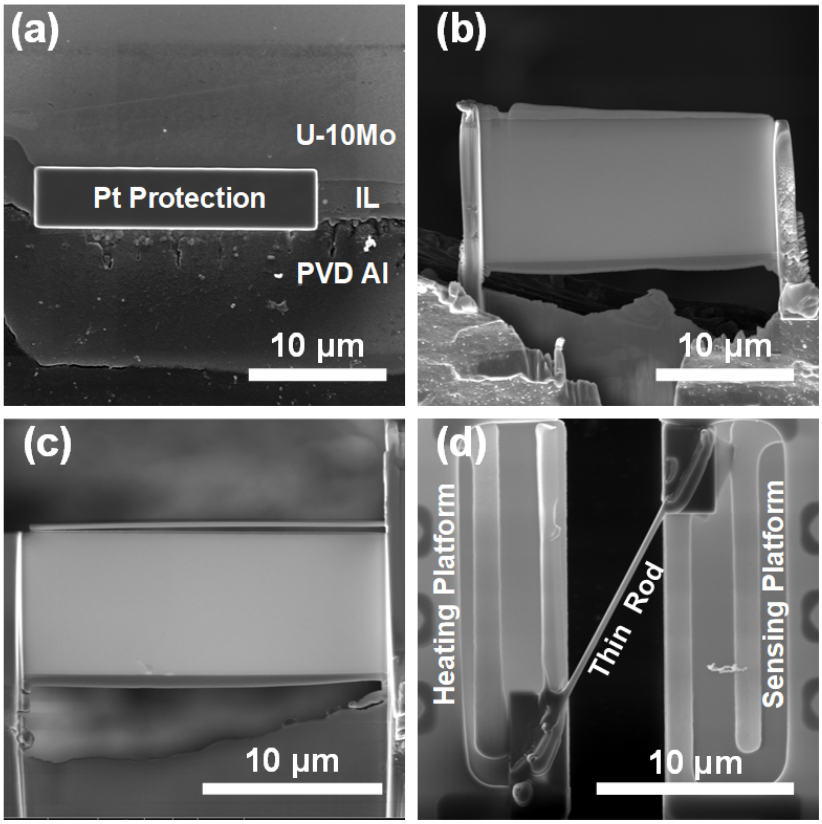

Figure 3: Preparation of the suspended bridge specimens from the Al-UMo IL induced by 80 MeV iodine ion irradiation: (a) Pt protection layer deposited on the Al-UMo IL formed near the ion beam center; (b) a lift-out and polished slice of the Al-UMo IL region; (c) a thin rod prepared from the lift-out and polished Al-UMo IL slice; (d) the thin rod specimen mounted on the measurement platform.

2.5. Measurement and Data Analysis

The measured thermal resistance (R_{bs}), which is the reciprocal value of the measured thermal conductance (G_{bs}), is contributed to by both the "bridge" part of the sample and the contact thermal resistance between the sample and the two platforms. Assuming that contact resistance is inversely proportional to the contact area with a coefficient C in m^2·K/W, the thermal conductivity of the measured material can be deduced after correcting for the contact resistance through linear regression of the measurement data of multiple thin rod specimens using the following equation:

$$R_{bs}dL_{contact} = \frac{LL_{contact}}{w}\frac{1}{k} + C \tag{3}$$

$$L_{contact} = \frac{L_h L_s}{L_h + L_s} \tag{4}$$

where, w, d, L, L_s, and L_h are dimensions defined in Fig. 2(b) and (c); and k is thermal conductivity of the measured material (Al-UMo IL in this study). The detailed deduction of the above equations can be found in Miao et al.'s previous work [16]. This approach to deduce thermal conductivity is thereafter referred to as the linear regression model in this study.

Compared to the previous study [16], some of the specimens prepared in this study have long contact lengths (i.e., L_s and L_h). When L_s and L_h are long enough, the assumption made in the deduction of the linear regression model is probably not valid. Hence, in order to ascertain the correctness of the linear regression model, a nonlinear form of the correlation between G_{bs} and k was deduced in this study. This model is referred to as the nonlinear regression model in this paper. With the detailed deduction given in the Supplementary Materials of this paper, the correlation has the following form:

$$G_{bs} = G_{bs}(C,k) = \frac{kwd}{L + \sqrt{Cwk}\left[coth\left(\sqrt{\frac{1}{Cwk}}L_h\right) + coth\left(\sqrt{\frac{1}{Cwk}}L_s\right)\right]} \tag{5}$$

where C in m^2·K/W is a coefficient related to the thermal conductance between the thin rod specimen and the two platforms, which has the identical definition as C in Equation 3. When

$L_h/\sqrt{Cwk}$ ~~$\sqrt{CwkL_h}$~~ and $L_s/\sqrt{Cwk}$ ~~$\sqrt{CwkL_s}$~~ are sufficiently small, using the Taylor series of $coth\ x = 1/x + O(x)$, Equation 5 can be reduced to Equation 3, as shown in the Supplementary Material. The least squares method (LSM) was then used to calculate the optimized values of k and C. Subsequently, the thermal conductivity (k) was derived using both linear and nonlinear regression models which are reported and compared in this study.

3. Results

3.1. Microstructure of Al-UMo Interaction Layer

In Fig. 5(a), it is obvious that an Al-UMo IL layer approximately 3~4 μm thick was formed on the PVD Al and UMo interface near the position irradiated by the ion beam center. The SEM image of the thin lamella sample prepared from the ion irradiated Al coated UMo foil is illustrated in Fig. 5(a). In both SEM and TEM (Fig. 5(a) and (c)), the Al-UMo IL shows a homogeneous microstructure except for some precipitates near the Al-IL and UMo-IL interfaces. The SEM-EDS scan across the Al-UMo IL (Fig. 5(b)) showed that the IL is composed of U, Mo, and Al with an approximately homogeneous composition of $(U_{0.8},Mo_{0.2})Al_{5.3}$ stoichiometry.

It is also worth mentioning that the implanted iodine-127 atoms are expected to deposit in either the UMo layer or near the IL-UMo interface in this irradiated sample, as predicted by SRIM simulation [33] (see Fig. 4). Considering the fact that the thin rod specimens were prepared near the center of the Al-UMo IL layer, a negligible amount of iodine-127 was deposited in the measured sample~~, which was also confirmed by SEM-EDS~~.

According to the U-Al phase diagram, if the stoichiometry parameter x in UAl_x exceeds 4, there is no well-defined crystalline intermetallic phase for U-Al compounds. Therefore, the Al-UMo IL investigated in this study is expected to be uniformly amorphous or to have an amorphous matrix with nanocrystalline inclusions [29]. The Al-UMo IL morphology was confirmed by TEM from a selected area diffraction pattern (SADP) of the Al-UMo IL region marked by the yellow circle in Fig. 5(a). The SADP collected is shown in Fig. 5(d), clearly indicating the characteristic pattern of an uniformly amorphous phase.

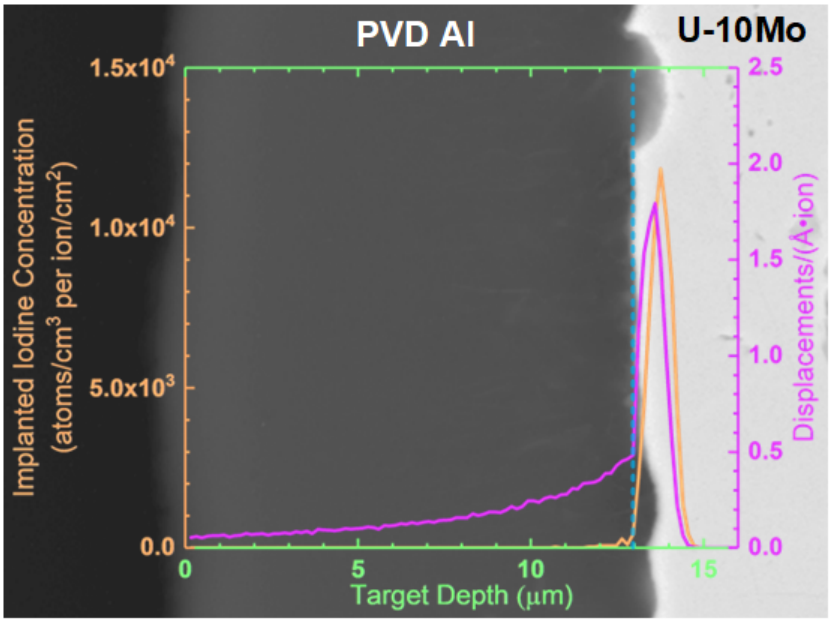

Figure 4: The SRIM predicted iodine distribution and ballistic displacement profiles in irradiated layered specimen overlaid with an SEM image of the layered sample before irradiation.

3.2. Thermal Conductivity of Al-UMo Interaction Layer

The thermal conductance values of the nine bridge specimens were measured at five different temperatures (300 K, 310 K, 320 K, 340 K, and 360 K). The linear regression model described in Equations 3 and 4 was first used to fit the measured thermal conductance data. An example of the linear fitting of the data collected at 360 K is given in Fig. 6(a). It is evident that the measurement data follow the linear regression model well, giving R^2 values of ~0.95 and uncertainty of ~0.5 W/mK in deduced thermal conductivity values. The thermal conductivity values derived from the linear regression model are also plotted in Fig. 6(b) as circles with error bars.

As mentioned earlier, a non-linear regression model was also developed for the suspended bridge system based on analytic solution of one-dimensional heat conduction equation. Using this non-linear regression model, the thermal conductivity of ion-induced Al-UMo IL can also be calculated based on the thermal conductance measurement results, which are also given in Fig. 6(b) in comparison to the linear regression results. Considering the overlapped error bars

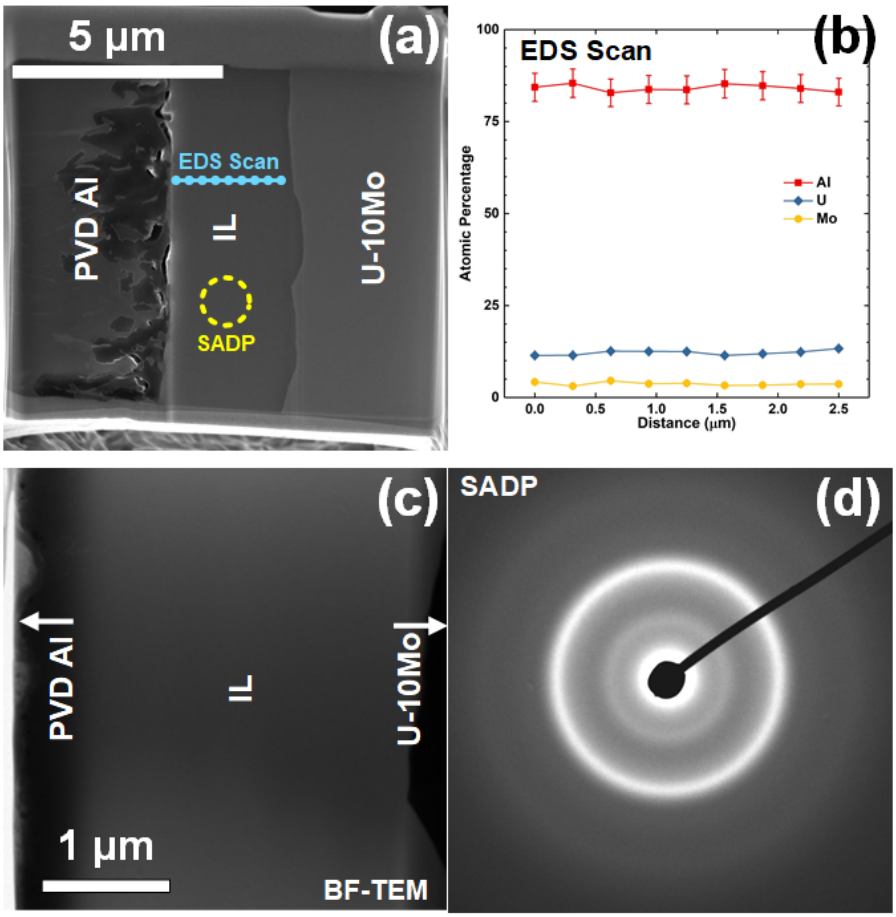

Figure 5: Microstructure of the Al-UMo IL investigated in this study: (a) an SEM image of the TEM lamella prepared for microstructure characterization; (b) elemental composition of the Al-UMo IL measured by SEM-EDS; (c) bright field (BF) TEM image of the Al-UMo IL showing the homogeneous structure; (d) selected area diffraction pattern (SADP) of the Al-UMo IL showing an amorphous structure.

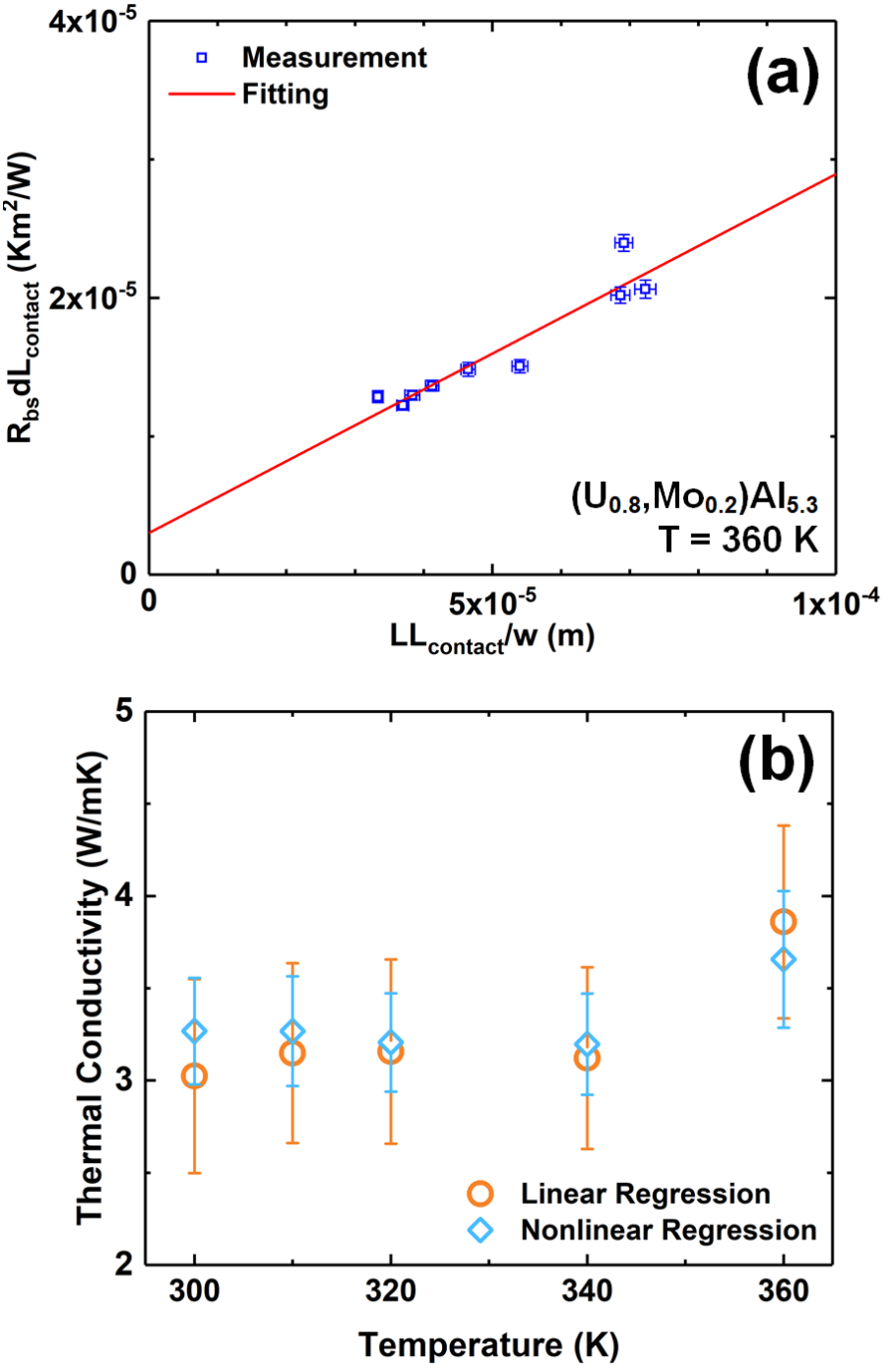

Figure 6: Deduction of thermal conductivity of the ion irradiation induced Al-UMo IL: (a) linear regression of the thermal conductivity at 360 K; (b) thermal conductivity determined by linear and nonlinear regression.

of the two sets of results, t~~T~~he thermal conductivity values deduced using the two methods are consistent. This demonstrates that the assumptions made in the derivation of the linear regression model are valid. The extraneous benefit of adopting the nonlinear regression model is that the measurement uncertainty is reduced from ~0.5 W/mK to ~0.3 W/mK.

4. Discussions

The thermal conductivity of the Al-UMo IL has been an unknown for the reactor conversion community. Some researchers suggested values slightly higher than the thermal conductivity of UMo fuel particles. According to some previous studies, the thermal conductivity of UAl_x ranges from approximately 4 to 8 W/mK [34, 35]. A recent density functional theory (DFT) calculation study reported the thermal conductivity of crystalline UAl_2, UAl_3, and UAl_4 [36]. Considering the IL is amorphous and contains Mo, these aforementioned measurements, or theoretical calculations, for crystalline UAl_x phases may help define an upper limit of the thermal conductivity of Al-UMo IL. For example, based on the thermal conductivity of UAl_x, Cho et al. suggested a value of ~3.6 W/mK [13]. In the present study, using high-energy heavy ion irradiation and an Al-coated monolithic UMo foil model system, an Al-UMo IL of amorphous $(U_{0.8},Mo_{0.2})Al_{5.3}$ was successfully produced, which is similar to the Al-UMo IL observed in in-pile irradiated UMo/Al fuel plates, in spite of the inverse irradiation direction. By employing the suspended bridge method, the thermal conductivity of the radiation-induced (U,Mo)Al_x IL with an amorphous structure was directly measured for the first time. The measured values are approximately 3~4 W/mK, within the 300 K to 360 K temperature range, which is slightly lower than those of crystalline UAl_x phases of Ref. [36].

In Ref. [16], suspended bridge method utilized in this study has been demonstrated to provide thermal conductivity measurement results that are consistent with results from conventional methods. Therefore, the thermal conductivity values measured by this novel method can be compared with thermal conductivity values in literature. In this study, the measured thermal conductivity of the Al-UMo IL is compared with the other two phases (i.e., UMo and Al) existing in UMo/Al dispersion fuel, as shown in Fig. 7. The UMo particle thermal conductivity in

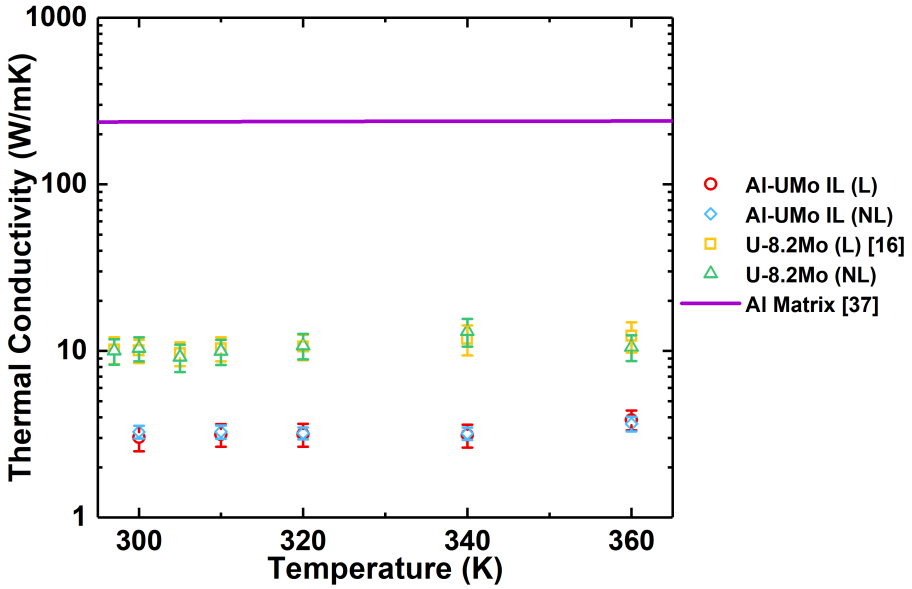

Figure 7: Comparison of the measured thermal conductivity of Al-UMo IL with those of UMo and Al ("L" indicates linear correlation, "NL" indicates nonlinear correlation).

Fig. 7 was measured using the suspended bridge method and found consistent with literature data, while the Al thermal conductivity was adopted from literature [37]. The measured thermal conductivity of Al-UMo IL is less than a third of that of typical UMo fuel particles [16] and is about two orders of magnitude lower than that of Al matrix [37], as shown in Fig. 7. Considering that Al-UMo IL contributes a significant fraction of the fuel meat volume at high burnup, the formation of Al-UMo IL and its accommodation of fission gases will considerably degrade the thermal conductivity of the UMo/Al dispersion fuel plate at high burnup. In Ye et al.'s fuel performance simulation work [38], the thermal conductivity of the UMo-Al IL was assumed to be 6 W/mK. If the IL thermal conductivity measured in this work (3~4 W/mK) is applied, calculated fuel meat thermal conductivity will be reduced and an increase in meat temperature is expected, providing other calculation parameters are kept the same. For example, by reducing this thermal conductivity from 6 W/mK to 3 W/mK, the DART-calculated peak fuel meat temperature (in °C) at the end of cycle increases by ~9% for a typical high-power irradiation.

The applicability of the suspended bridge method for atomized and annealed UMo particles have been demonstrated in Miao et al.'s previous work [16]~~[37]~~. It is the first time that the thermal conductivity of Al-UMo IL produced by ion irradiation was directly measured, using the suspended bridge method. The thermal conductivity of Al-UMo IL has not been directly measured in the past, mainly because the IL is so small that a conventional method such as the laser flash method cannot be utilized. The present study demonstrates that the suspended bridge method is a valuable tool in measuring the thermal conductivity of microstructures formed in irradiated materials that otherwise cannot be determined by conventional methods. Other measurements are to be performed in the future, including Al-U_3Si_2 IL and amorphous U_3Si_2 induced by heavy ion irradiation, as well as some in-pile irradiated samples.

5. Conclusions

In this study, a model system consisting of a UMo substrate coated with Al was irradiated by high-energy iodine ions up to a fission density equivalent of 3.18×10^{20} fissions/cm^3 to induce Al-UMo IL. The microstructure of Al-UMo IL was investigated by a series of techniques, showing

that the formed IL is homogeneous $(U_{0.8},Mo_{0.2})Al_{5.3}$ with an amorphous structure, similar to the Al-UMo IL observed in in-pile irradiated UMo/Al fuel plates. The suspended bridge method was used to directly measure the thermal conductivity of the Al-UMo IL. The results indicated the thermal conductivity of the Al-UMo IL is approximately 3~4 W/mK at temperature ranging from 300 K to 360 K, compared to approximately 10~20 W/mK of the UMo alloy and 200~300 W/mK of the Al matrix. These results prove that the Al-UMo IL is the one of the major sources of the degradation of the thermal conductivity of UMo/Al dispersion fuel. This study demonstrates the applicability of the suspended bridge method to nuclear materials research.

6. Acknowledgments

This work was sponsored by the U.S. Department of Energy, Office of Material Management and Minimization in the U.S. National Nuclear Security Administration Office of Defense Nuclear Nonproliferation under Contract DE-AC02-06CH11357. S.S. acknowledges support from the National Science Foundation under Grant NSF-CBET-17-06854. The IVEM related work was supported by the U.S. Department of Energy, Office of Nuclear Energy under DOE Idaho Operations Office Contract DE-AC07-051D14517 as part of a Nuclear Science User Facilities experiment. The TUM efforts were supported by a combined grant (FRM1318) from the Bundesministerium für Bildung und Forschung (BMBF) and the Bayerisches Staatsministerium für Wissenschaft, Forschung und Kunst (StMWFK) and by the European Commission in the framework of HORIZON 2020 through Grant Agreement 661935 in the HERACLES-CP project.

7. Data Availability Statememt

The raw/processed data required to reproduce these findings cannot be shared at this time as the data also forms part of an ongoing study.

References

[1] A. Travelli, The US RERTR program status and progress, Technical Report, Argonne National Lab., 1998.

[2] J. L. Snelgrove, G. Hofman, C. Trybus, T. Wiencek, Development of very-high-density fuels by the RERTR program, Technical Report, Argonne National Lab., 1996.

[3] Y. S. Kim, G. Hofman, J. Rest, A. Robinson, Journal of Nuclear Materials 389 (2009) 443–449.

[4] G. Hofman, J. Snelgrove, S. Hayes, M. Meyer, Progress in development of low-enriched U-Mo dispersion fuels., Technical Report, Argonne National Lab., IL (US), 2002.

[5] Y. S. Kim, in: R. J. Konings (Ed.), Comprehensive Nuclear Materials, Elsevier, Oxford, 2012, pp. 391 – 422.

[6] Y. S. Kim, G. Hofman, Journal of Nuclear Materials 419 (2011) 291–301.

[7] G. Hofman, M. Meyer, J. Snelgrove, M. Dietz, R. Strain, K. Kim, Initial assessment of radiation behavior of very-high-density low-enriched-uranium fuels., Technical Report, Argonne National Lab., IL (US), 1999.

[8] P. Lemoine, D. Wachs, in: Proc. Inter. Meeting on RERTR-2007, Citeseer, pp. 23–27.

[9] E. Koonen, H. Guyon, P. Lemoine, C. Jarousse, D. Wachs, J. Stevens, in: Proc. Inter. Meeting on RERTR-2009, pp. 1–5.

[10] A. Leenaers, S. Van den Berghe, E. Koonen, C. Jarousse, F. Huet, M. Trotabas, M. Boyard, S. Guillot, L. Sannen, M. Verwerft, Journal of Nuclear Materials 335 (2004) 39–47.

[11] H. J. Ryu, Y. S. Kim, G. Hofman, Journal of Nuclear Materials 385 (2009) 623–628.

[12] S. Van den Berghe, W. Van Renterghem, A. Leenaers, Journal of Nuclear Materials 375 (2008) 340–346.

[13] T. W. Cho, Y. S. Kim, J. M. Park, K. H. Lee, S. Kim, C. T. Lee, J. H. Yang, J. S. Oh, D.-S. Sohn, Journal of Nuclear Materials 501 (2018) 31–44.

[14] T. K. Huber, H. Breitkreutz, D. E. Burkes, A. J. Casella, A. M. Casella, S. Elgeti, C. Reiter, A. B. Robinson, F. N. Smith, D. M. Wachs, et al., Journal of Nuclear Materials 503 (2018) 304–313.

[15] D. E. Burkes, T. K. Huber, A. M. Casella, Journal of Nuclear Materials 473 (2016) 309–319.

[16] Y. Miao, M. C. Rajagopal, K. Valavala, K. Mo, Z.-G. Mei, S. Bhattacharya, L. Jamison, S. Sinha, A. M. Yacout, Journal of Nuclear Materials 527 (2019) 151797.

[17] L. Shi, D. Li, C. Yu, W. Jang, D. Kim, Z. Yao, P. Kim, A. Majumdar, Journal of heat transfer 125 (2003) 881–888.

[18] L. Shi, Q. Hao, C. Yu, N. Mingo, X. Kong, Z. L. Wang, in: ASME 2004 Heat Transfer/Fluids Engineering Summer Conference, American Society of Mechanical Engineers, pp. 457–461.

[19] M. Ghossoub, K. Valavala, M. Seong, B. Azeredo, K. Hsu, J. Sadhu, P. Singh, S. Sinha, Nano letters 13 (2013) 1564–1571.

[20] N. Wieschalla, A. Bergmaier, P. Böni, K. Böning, G. Dollinger, R. Großmann, W. Petry, A. Röhrmoser, J. Schneider, Journal of nuclear materials 357 (2006) 191–197.

[21] H. Palancher, N. Wieschalla, P. Martin, R. Tucoulou, C. Sabathier, W. Petry, J.-F. Berar, C. Valot, S. Dubois, Journal of Nuclear Materials 385 (2009) 449–455.

[22] H. Chiang, T. Zweifel, H. Palancher, A. Bonnin, L. Beck, P. Weiser, M. Döblinger, C. Sabathier, R. Jungwirth, W. Petry, Journal of Nuclear Materials 440 (2013) 117–123.

[23] R. Jungwirth, T. Zweifel, H.-Y. Chiang, W. Petry, S. Van den Berghe, A. Leenaers, Journal of nuclear materials 434

(2013) 296–302.

[24] B. Ye, L. Jamison, Y. Miao, S. Bhattacharya, G. Hofman, A. Yacout, Journal of Nuclear Materials 488 (2017) 134–142.

[25] Y. Miao, J. Harp, K. Mo, S. Zhu, T. Yao, J. Lian, A. M. Yacout, Journal of Nuclear Materials 495 (2017) 146–153.

[26] Y. Miao, T. Yao, J. Lian, S. Zhu, S. Bhattacharya, A. Oaks, A. M. Yacout, K. Mo, Scripta Materialia 155 (2018) 169–174.

[27] Y. Miao, J. Harp, K. Mo, Y. S. Kim, S. Zhu, A. M. Yacout, Journal of Nuclear Materials 503 (2018) 314–322.

[28] Y. Miao, J. Harp, K. Mo, Z.-G. Mei, R. Xu, S. Zhu, A. M. Yacout, Journal of Nuclear Materials 518 (2019) 108–116.

[29] J. Shi, H. Breitkreutz, W. Petry, C. Onofri, H. Palancher, D. Drouan, X. Iltis, in: Proceedings of European Research Reactor Conference RRFM 2019.

[30] J. Shi, H. Breitkreutz, W. Petry, in: Proceedings of European Research Reactor Conference RRFM 2018.

[31] H. Breitkreutz, A. Heldmann, J. Hingerl, R. Jungwirth, J. Shi, W. Petry, Journal of Nuclear Materials 507 (2018) 276–287.

[32] D. E. Burkes, A. J. Casella, A. M. Casella, Journal of Nuclear Materials 478 (2016) 365–374.

[33] J. F. Ziegler, M. D. Ziegler, J. P. Biersack, Nuclear Instruments and Methods in Physics Research Section B: Beam Interactions with Materials and Atoms 268 (2010) 1818–1823.

[34] T. Jones, K. Street, J. Scoberg, J. Baird, Canadian Metallurgical Quarterly 2 (1963) 53–72.

[35] A. Jesse, G. Ondracek, F. Thümmler, Powder Metallurgy 14 (1971) 289–297.

[36] Z.-G. Mei, Y. S. Kim, A. M. Yacout, J. Yang, X. Li, Y. Cao, Materialia 4 (2018) 449–456.

[37] Y. S. Touloukian, R. Powell, C. Ho, P. Klemens, Thermophysical properties of matter-the tprc data series. volume 1. thermal conductivity-metallic elements and alloys, Technical Report, Thermophysical and Electronic Properties Information Analysis Center, 1970.

[38] B. Ye, G. Hofman, A. Leenaers, A. Bergeron, V. Kuzminov, S. Van den Berghe, Y. Kim, H. Wallin, Journal of Nuclear Materials 499 (2018) 191–203.